INFLUENCE OF DESIGN AND LOADING ON THE MECHANICAL BEHAVIOUR OF THICK COMPOSITE LUGS

Carolin Werchner[1], Dr. Tamas Havar[1], Prof. Dr. Klaus Drechsler[2],
[1] EADS Deutschland GmbH - Innovation Works, Willy-Messerschmitt-Str., 81663 Munich
[2] TU München, Lehrstuhl für Carbon Composites, Boltzmannstr. 15, 85748 Garching

Abstract

This paper focuses on the investigation of the mechanical behaviour of single pin loaded, thick composite laminates. These so called thick composite lugs play an important role for load introduction structures in today's aircraft design. In order to obtain general information about the failure behaviour of composite lugs a static test program using generic specimens is presented. Different laminate layups are investigated as well as different lug geometries. Especially the failure mode and the failure loads for first ply failure and last ply failure of the different lug configurations are used for the derivation of general design guidelines.

Keywords: Composite lugs, bolted joints, load introduction structures, composite failure.

1. INTRODUCTION

The use of composites in aircraft design is well- known all over the world. As composites have been used in commercial airplanes for more than 30 years a lot of experience has been amassed, thereby. At the beginning, composites were mainly used for large 2-dimensional non load carrying panels. Over the years, composite components grew in complexity by integrating reinforcing elements such as e.g. a wing box with composite stringers. The know-how about these structurally more relevant components grew also. Today, the ratio of composites in structural weight in aircraft design has exceeded 50% and accordingly the need for a more integral design has increased, too. Thus, composites are even used for locally highly loaded components in order to bring the loads from thick structures into thinner, plane skin structures. The challenge now is to establish a well-founded knowledge on these complex thick structures as well. [1]

The most difficult point about highly loaded composite structures is the load introduction respectively the joining with other structural components. There is a certain amount of well-understood joining techniques for thin composite structures which has been developed. But these design methods are not necessarily applicable on thick composite laminates e.g. used in load introduction structures. For highly loaded thick aircraft structures design rules only exist for metal materials. Hence, there is a need to investigate thicker composite structures in general.

The approach within this work aims to investigate composite load introduction structures using generic objects. Basically, a virtual testing approach is conducted, whereby the focus of this paper lies on the testing activities. Thus, a test setup is presented and the results are discussed in detail.

2. COMPOSITE LOAD INTRODUCTIONS

This investigation focuses on composite load introduction structures i.e. highly loaded bolted joints. While riveted joints are widely-used – considering e.g. thousands of rivets for the fuselage joints – single pin joints can be found only in few composite aircraft structures. Composite single pin joints are solely used at local load concentrations in thick composite structures. Those single pin joints can be found for example at the aircraft wing looking at the A340 spoiler manufactured by FACC (FIGURE 1). Other current applications are helicopter rotor heads or the A400M vertical tail plane [2][3][4].

The design of composite single pin joints can be developed in two main ways: composite lugs and composite loops. While composite loops use fibre strands around the pin for carrying particularly high tensile forces, composite lugs are thick composite plates with a hole in it (FIGURE 2). Thicknesses of up to 35mm are considered within this work as these are needed to cover most of the requirements for aircraft design. Anyway, the reader should keep in mind that even thicker structures of up to 90mm wall thickness – so called ultra thick laminates (UTL) – do exist [5]. But these ULT are not analysed in this work due to the fact that they are not in use for today's commercial airplanes. Further information about composite loops is to be found in literature, such as [6][7][8].

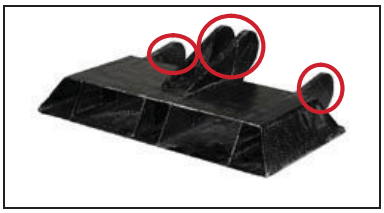

FIGURE 1. A340 spoiler with composite lugs [4]

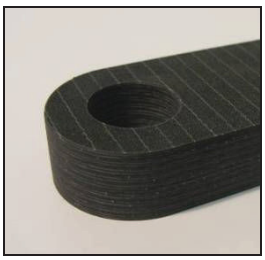

FIGURE 2. Composite lug - a thick laminate with a hole

3. FAILURE BEHAVIOR

Composite materials exhibit a strongly different failure behaviour compared to metals. The reason for that is not only the anisotropic material properties of composites that lead to a failure that depends on the load direction, but the brittle material behaviour that is not able to show plastic deformations. Therefore, composite structures fail by various failure modes which are mainly divided in inter fibre failure and fibre failure. The failure mode of inter fibre failure can be subdivided into delamination describing the failure of the interface between two plies, and fibre matrix interface failure as well as pure matrix cracking within a ply. Examples for composite failure are shown in FIGURE 3 and in literature [6].

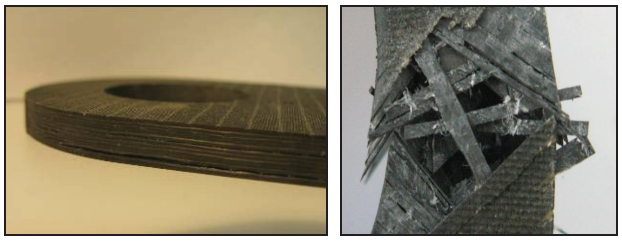

FIGURE 3. Delamination, example for inter fibre failure (left), fibre failure (right)

The investigation of composite failure on a larger scale leads to the differentiation between first ply failure and total failure for a specific component. First ply failure represents a damage initiation event which is usually the onset of inter fibre failure in any ply. When loads are further increased on that damaged component other plies fail until external forces cannot be increased any more. At that status total failure or last ply failure occurs. This failure event represents the failure of the remaining load carrying plies which is to be considered as the catastrophic failure of the structure. The failure behaviour of thick composite structures will be presented in this paper.

4. TESTING APPROACH

For a better understanding of the failure behaviour of thick composite load introduction lugs, a series of tests on thick composite lugs has been conducted. The aim of the test series was to investigate the process of failure including the failure mode as well as the loads at first and last ply failure of different composite lug configurations. The different configurations distinguish themselves by the lug geometry and laminate layup. A simple specimen geometry was chosen in order to gain further information about the overall failure behaviour of thick composite lugs in general.

4.1. Specimens

The tested specimen can be classified by the laminate layup. A quasi-isotropic (QI) layup (25|50|25) was compared with a (50|40|10) layup. Both layups consist of 128 plies resulting in a total thickness of about 34mm. The quasi-isotropic specimens were manufactured with Saertex non crimp fabric material with HTA fibres. The biaxial textile material was chosen in order to provide the comparability to standard material in aircraft industries. The (50|40|10) specimens were manufactured using the same biaxial textile material. Moreover, these specimens use unidirectional fabric Hexcel G1157 for providing the additionally used fibres in 0°-direction.

The infusion process has been chosen to be a Vacuum Assisted Process (VAP) using the Hexcel RTM6 epoxy resin. The VAP uses solid tools only for one side of the plate a semipermeable membrane on the other side which is quite beneficial as costs for tools are omitted and the pressure of an autoclave is not necessary. This infusion process was used due to the fact that it is a well known process for the aircraft industry and it gives a lot of freedom of manufacturing feasibility for future composite lug applications.

The test specimens (FIGURE 4) were cut out of large, thick plates using water jet cutting. Water jet cutting is well-suited for the machining process as it is able to cut the required contours precisely in a short time. The holes were additionally milled in order to get a even higher tolerance of ±0.05mm.

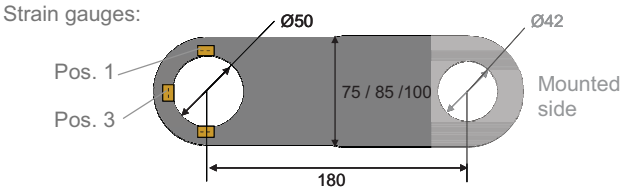

FIGURE 4. Specimen geometry (tested lug left)

The lug diameters and distances between the lug centre points are constant for all configurations. The geometry of the tested lug side was changed by varying the ratio between the outer radius r_a and inner radius r_i (= bolt diameter) from 1.5 and 1.7 to 2.0 with a constant bolt diameter of r_i = 50mm. Especially the r_a/r_i = 2.0 configuration seems to be close to common aircraft geometries. Thus, the outer radius r_a varies from 75mm over 85mm to 100mm.

4.2. Test Setup

The tensile test were conducted at EADS Innovation Works for the all specimens with a ratio of r_a/r_i=1.5 and r_a/r_i=1.7. Due to the increased failure load, the tests for the r_a/r_i = 2.0 specimen configuration were conducted at the facilities of the University of Armed Forces in Munich (FIGURE 5). The testing speed was 1 mm/min for all specimens.
The lugs were mounted with fork head brackets made of steel. Furthermore, steel bolts were used with a loose fit to the lugs. No bushes were used i.e. that there was no additional support for the lug such as a collar or a flange form a bushing. So, the number of influencing clamp parameters was reduced and the unaffected failure behaviour of the lugs was tested.

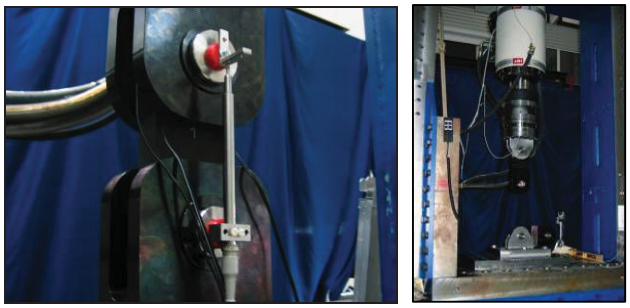

FIGURE 5. Tensile test rig (University of Armed Forces, Munich)

4.3. Instrumentation

Different instrumentation approaches were chosen in order to get comprehensive data about the deformation status of the specimens. The most important instrumentation is the strain gauge approach which was used for all tests and will be discussed in more detail. Additionally, some of the samples were measured using position sensors or the greyscale correlation approach *Aramis*. The latter one was used to gain a continuous strain distribution all over the specimen and get further information about the highest loaded areas thereby.

4.3.1. Strain Gauges

Due to their very precise measurement results strain gauges are commonly used for strain measurement. As the strain results are directly coupled to the testing machine, the correlation to the corresponding loads and stresses can be established easily. So, the structural stiffness can be determined directly by using the stress-strain curves. These stress-strain curves respectively the load-strain curves can be used in order to observe stiffness discontinuities representing failure events.

A disadvantage of strain gauges for measuring composite structures is the dependency on the top layer of the laminate. A strain gauge will always stop giving strain data whenever the top layer fails exactly at the strain gauge position. But that does not necessarily have to be equivalent to the failure of the underlying layers. Assuming an approximately constant strain distribution over the lug thickness, the strain results of a strain gauge are valid solely as long as it delivers data. After the failure of the strain gauge respectively the failure of the top layer no assumption about the damage condition of the whole lug specimen can be made.

Furthermore, one has to be careful when considering not only the rough order of magnitude of the strain results. As the strain gauges are bonded manually to the specimens, small misalignments considering the orientation of the strain gauge in relation to the fibre direction are always possible. Therefore, the measured values are to be considered as local values and not as global values. The position of a strain gauge in relation to the fibre direction and the laminate stacking should be kept in mind for the interpretation of results.

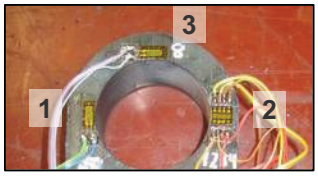

FIGURE 6. Distribution of strain gauges including the numbering of the strain gauge positions

However, the wide spread usage of strain gauges is definitely reasonable for thick laminates as well. For the instrumentation in this test series three strain gauges were used per specimen having two at the lateral side directed in load direction and having one strain gauge in the front directed transverse to the loading (FIGURE 6). Additionally, for one specimen per configuration a single strain gauge at a lateral position was replaced by a series of strain gauges (FIGURE 6, strain gauges at position 2). Using several strain gauges over one net section gives the opportunity to gain information about the strain distribution in that net section area. Linear strain gauges with a measuring grid area of 2.8mm x 6mm were used for all positions except the series of strain gauges.

4.4. Test matrix

The following table gives an overview over the statically tested specimens. The specimens vary within their geometry and their laminate layup. The specimen thickness is approx. 34mm for all samples.

Radius Rratio r_a/r_i	Laminate Layup	Number of Specimen
1.5	QI	6
1.7	QI	6
2.0	QI	6
1.5	(50|40|10)	7
1.7	(50|40|10)	6

TABLE 1. Test matrix

5. RESULTS

The evaluation of the test results is to be divided into two categories: first of all, the influence of the laminate layup on the failure behavior will be discussed. Furthermore, the influence of the lug geometry will be investigated in more detail with attention to the radius ratio.

5.1. Influence of the Laminate Layup

It is mandatory for the comparison of different laminate layups to have test specimen with identical geometries in order to isolate the influence of the laminate layup. According to TABLE 1 two different geometries – with a radius ratio of 1.5 and 1.7 – are available but for reasons of simplification all results are shown using the example of r_a/r_i=1.7. However, the findings for the r_a/r_i=1.5 test series show basically similar results.

The main difference between the specimens with the above mentioned quasi-isotropic layup and the ones with the (50|40|10) layup is the global failure mode. The (50|40|10) specimens all fail due to a bearing respectively a shear-out failure (FIGURE 7). This failure mode appears when two load conditions are superimposed: Firstly, high

compression loads are transmitted from the bolt to the inner surface of the lug and secondly, inner forces directed transverse to the external tensile loads are induced via shear and lateral contraction. If a shear-out failure occurs, a distribution of loads from the near bolt area via the lateral parts of the lug specimens farther into the main structure has not been possible.

The global failure mode found for all quasi-isotropic specimens is tension failure at net section (FIGURE 8). This failure mode is caused by high tensile forces that are distributed from the lug into the lateral part of the specimen. Even though one side of the QI lug specimens always fails first, both sides are damaged strongly.

FIGURE 7. Centric shear failure of (50|40|10) sample

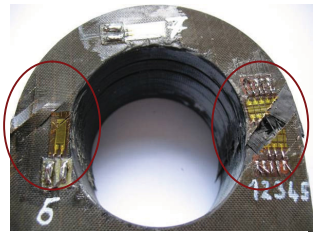

FIGURE 8. Lateral tension failure at smallest net section of QI-specimen

For the quasi-isotropic specimens rupture behaviour is detectable. That means that the lug is divided into blocky subsections which are caused by few but large delaminations (FIGURE 10). For some of the specimens, these subsections even completely break away from the residual specimen (FIGURE 11, left). In contrast to that, the (50|40|10) specimens basically do not separate in subsections even though large delaminations can be found, too. But these delaminations are smaller considering the delaminated area and more distributed over the specimen thickness (FIGURE 9). Furthermore, these delaminations do not lead to an opening between the layers as it can be found for the quasi-isotropic specimen, compare FIGURE 9 and FIGURE 10. Thus, the failure of the (50|40|10) specimen seems to be the more gradual and therefore the preferred failure characteristic. The number of delaminations at the fracture location is about the same for both layup configurations (FIGURE 9 and FIGURE 10).

FIGURE 9. (50|40|10) specimen, r_a/r_i = 1.7

FIGURE 10. QI specimen, r_a/r_i = 1.7

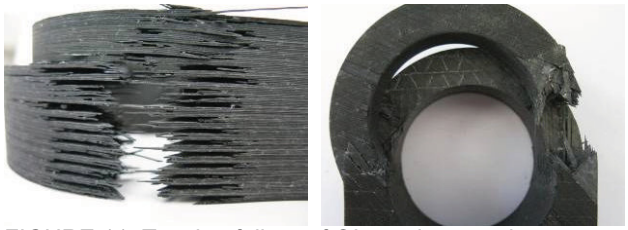

FIGURE 11. Tension failure of QI specimen: sub-groups of 4 plies (left) disrupted subsection (right)

As the quasi-isotropic layup is made up of much smaller packages of the recurring stacking sequence (+45/-45 0/90 -45/+45 90/0), failure occurs in a regular pattern. There is a regular distribution of sub-groups that consist of 4 plies each, see FIGURE 11. It can be assumed that it is always the interface between the above mentioned package of a stacking sequence that fails and the interface in the middle of the stacking sequence.

The most loaded area – which is the considered as the main damaged area – can be found not only by investigation of the fracture mode but by interpretation of the load-strain curves (FIGURE 13 - FIGURE 15). Here, the abscissa shows the strain measured at the strain gauge at position 1 or 3. The ordinate represents the load applied by the testing machine. The different specimen configurations can be distinguished by the different colours blue, green and red for the three different radius ratios 1.5, 1.7 and 2.0. The pale coloured curves are the test results of each tested specimen (at least 6 per configuration). The darker curves are fitting curves for each lug specimen configuration. The curves are always valid for one specific laminate layup that is mentioned within the title of the figure.

The determination of the most critical area of the specimen can roughly be made by looking at the load-strain curves for the two different strain gauge positions that are investigated. The highest strain values of the (50|40|10) layup appear at strain gauge position #3 which is directed transverse to the load direction (FIGURE 13 and FIGURE 14). The high strain values of more than 1% are a sign for large deformations caused by stiffness degradation due to failure. Shear forces resulting from the applied tension might be responsible for the large deformations and finally for the centric, total lug failure.

Considering the damage of the quasi-isotropic specimen the highest strain values are to be found at strain gauge position #1 (lateral), see FIGURE 12 and FIGURE 15. Again this is the main fracture area of the specimen. As the strain gauges are directed axial to the loading direction this failure can be considered as tensile failure.

Looking at the load-strain curves in terms of the qualitative behaviour, one can see that the load increase for the quasi-isotropic layup is basically linear (FIGURE 12 and FIGURE 15) whereas the stiffness of the (50|40|10) layup at the most damaged area at position 3 shows a clear nonlinear behaviour (FIGURE 14). One can assume that again – as mentioned above – the (50|40|10) layup has the softer, more gradual failure behaviour.

The further comparison of the two different laminate layups leads to the quantitative comparison of failure loads. Failure loads for the quasi-isotropic layup are slightly above the ones of the (50|40|10) layup, see FIGURE 16. First ply failure as well as total failure occurs at lower load levels for the (50|40|10) layup. It is important to keep in mind that the total failure loads are the maximum loads the specimen could carry. The first ply failure loads are estimated by looking for discontinuities respectively nonlinearities within the loads-strain curves. Additionally, the loads at audible crack events were taken into consideration for the estimation of first ply failure loads.

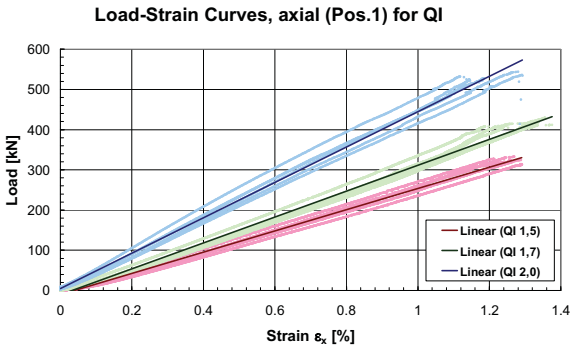

FIGURE 12. Load-strain curves for QI layup (axial)

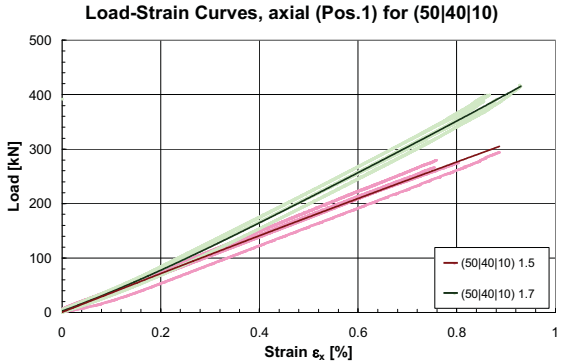

FIGURE 13. Load-strain curves for (50|40|10) layup (axial)

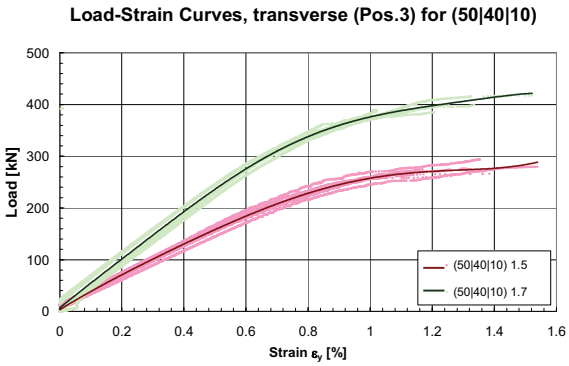

FIGURE 14. Load-strain curves for (50|40|10) layup (transverse)

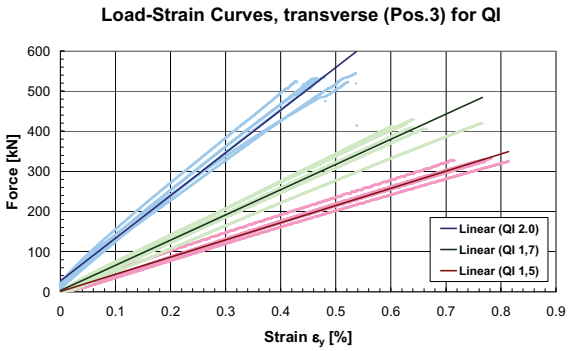

FIGURE 15. Load-strain curves for QI layup (transverse)

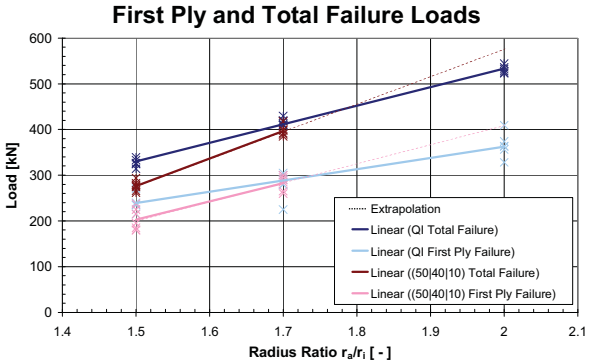

FIGURE 16 Failure loads for QI and (50|40|10) layup

5.2. Influence of Radius Ratio r_a/r_i

As described in section 4.1 three different radius ratios r_a/r_i were tested in order to provide information about geometries that appear close to today's aircraft design. While the laminate layup showed a dominant influence on the failure mode in section 5.1, the test results also showed that there is a major influence of the lug geometry on the failure load (FIGURE 16) together with a minor, but clear influence on the failure mode.

Investigating the failure mode in more detail, the (50|40|10) specimens fail for a radius ration r_a/r_i = 1.5 with pure shear failure and for r_a/r_i = 1.7 some of the specimen fail with a combination between shear failure and tension failure. Even though the shear failure is still dominant, a certain amount of fibres – especially within the outer plies – fail at the lateral side with the smallest net section (FIGURE 17). Therefore, one can see that there is a tendency to fail in tension failure for any laminate layup if only the radius ratio is high enough.

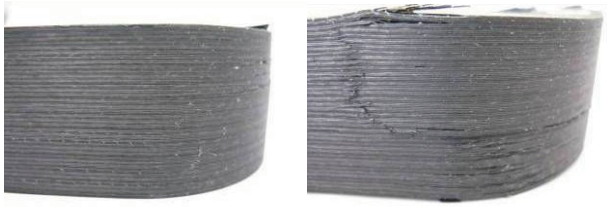

FIGURE 17. Lateral view on (50|40|10) specimen: r_a/r_i = 1.5 (left), r_a/r_i = 1.7 (right)

At the same time this means that there is – up to a certain amount – a redistribution of loads into the lateral parts of the r_a/r_i = 1.7 specimen. This is beneficial due to the fact that now almost the same load level for first and total failure is reached. Without having tested it, one can assume that for a larger radius ratio than r_a/r_i = 1.8 the structure is able to bear even more load for the (50|40|10) layup than for the quasi-isotropicl layup, see dotted line in FIGURE 16. The question whether the extrapolated curve can be assumed to be linear, should be confirmed or corrected after further testing efforts.

In contrast to the (50|40|10) layup the quasi-isotropic layup does not change the failure mode in general when increasing the radius ratio. But it can be noticed that the blocky subsections mentioned in section 5.1 tend to break off the residual structure especially for smaller radius

ratios r_a/r_i. For larger radius ratios r_a/r_i a larger number of load carrying plies remains even after first ply failure and therefore the rupture behaviour is less distinctive, compare and FIGURE 11 and FIGURE 18.

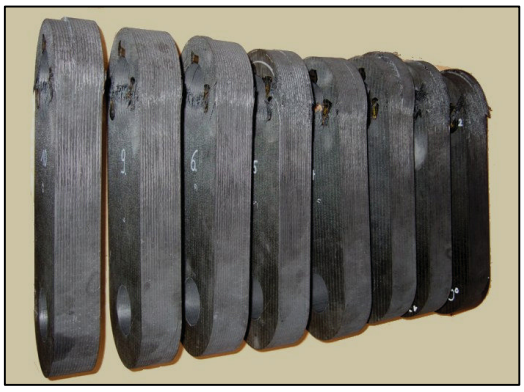

FIGURE 18 Tested specimen: QI layup, $r_a/r_i = 2.0$

The comparison between the different geometric lug configurations for the quasi-isotropic specimens leads to the further investigation of failure loads. In FIGURE 16, there is a linear correlation between the failure loads and the radius ratio. As a first estimation this correlation can be described by the following equations (1) and (2):

Failure load for first ply failure:

(1) $$F_{fail}^{first} \approx 245kN \cdot \left(\frac{r_a}{r_i}\right) - 130kN$$

Failure load for total failure:

(2) $$F_{fail}^{total} \approx 406kN \cdot \left(\frac{r_a}{r_i}\right) - 280kN$$

But the reader should keep in mind that these equations are only valid for quasi-isotropic specimen with a thickness of 34mm loaded by axial tensile forces. The derivation of similar equations for the (50|40|10) layup is not possible at the moment as it requires more data input either from testing or from numerical analysis.

6. TRANSFER TO NUMERICAL INVESTIGATION

As mentioned at the beginning of this paper the author focuses on both experimental and numerical investigation on composite load introduction structures. The presented experimental results provide a basis for finite element analyses with respect to the model validation. After validation of the numerical material model it is possible to establish a virtual testing approach for composite lugs. A greater number of geometric parameters can be investigated with this approach.

7. CONCLUSION AND OUTLOOK

This paper showed an overview over failure modes and failure loads for different composite lug configurations under static tensile loads. The different lug configurations varied with respect to the laminate layup and the ratio between outer and inner radius of the tested lug.

It was shown that the (50|40|10) laminate layup fails by shear-out failure, especially for a small radius ratio. For a larger radius ratio, loads were distributed better into the lateral parts of the specimen, and therefore, the failure mode inclined towards a tension failure at the net section. But the main failure event was still shear-out failure for all tested specimen.

The quasi-isotropic laminate failed by tension failure at the net section for all tested specimens. Large delaminations and separation of disrupted subsections were observed. Furthermore, a linear correlation between the failure load and the radius ratio r_a/r_i was found.

The failure behaviour of the (50|40|10) can be considered as the more favourable one due to the fact that both the stiffness degradation and the occurrence of fibre fracture are more gradual for this layup than for the quasi-isotropic layup. On the other side, the tested quasi-isotropic specimen were able to carry higher loads until last ply failure. Therefore, it is recommended to use quasi-isotropic laminate layups whenever very small radius ratios are used. In case of large radius ratios for the (50|40|10) layup the failure loads are expected to be even higher than for the quasi-isotropic laminate layup. However, this expectation should be proved in future via further testing activities.

Other reasonable investigation could deal with other laminate thicknesses and lug geometries. Furthermore, results of numerical investigations should be associated to the presented investigation for a sound validation of the numerical model and further lug investigations.

8. ACKNOWLEDGEMENT

Major parts of this work were performed in cooperation in the framework of a subcontract by Airbus Operations GmbH for the German national funded project HIGHER-TE (High Lift Enhanced Research – Trailing Edge, LuFo IV 2nd call). Furthermore, this work was supported by the University of Armed Forces, Munich, carrying out parts of the tests, and by the Technical University, Munich, supporting this work in general.

9. LITERATURE

[1] Niu, M. Ch.-Y. : “Airframe Structural Design“, 1995
[2] Pfaller, R., Ahci Ezgi, E.: „Einfluss von Geometrie und Materialparametern auf die Festigkeit von Verbindungen in Hubschrauberstrukturen“, Deutscher Luft- und Raumfahrtkongress 2008
[3] Longeru, M., Grund, V., Meyfarth, D.: “Efficient, semi-automated property definition on complex composite structure FE models on the example of detailed test specimen models for accurate test prediction”, Deutsche Simulia Konferenz 2010
[4] http://www.compositesworld.com/articles/airbus-a340-carbon-composite-spoiler-made-with-rtm, 01.08.2011
[5] Zimmermann, K., Zenkert, D., Siemetzki, M.: “Testing and analysis of ultra thick composites”, Composites Part B: Engineering, Vol 41, 2010, pp 326-336
[6] Schürmann, H.: „Konstruieren mit Faser-Kunststoff-Verbunden“, Springer-Verlag, 2. Auflage, 2007
[7] Havar, T.: „Beitrag zur Gestaltung und Auslegung von 3D-verstärkten Faserverbundschlaufen“, Dissertation, Universtiät Stuttgart – Institut für Flugzeugbau, 2007
[8] Bansemir, H.: „Schlaufenartige Krafteinleitungs-elemente in FVW-Bauweise“, Seminar „Hoch-leistungsstrukturen im Leichtbau“, Munich, 2004